

Influence of high temperature exposure on the mechanical behavior and microstructure of 17-4 PH stainless steel

JUI-HUNG WU, CHIH-KUANG LIN*

Department of Mechanical Engineering, National Central University, Chung-Li 32054, Taiwan
E-mail: t330014@cc.ncu.edu.tw

The mechanical behavior and microstructural evolution of 17-4 PH stainless steels in three conditions, i.e. unaged (Condition A), peak-aged (H900) and overaged (H1150), exposed at temperatures ranging from 200 to 700°C were investigated. The high-temperature yield strength of each condition decreased with an increase in temperature from 200 to 400°C except for Condition A at 400°C with a longer hold time where a precipitation-hardening effect occurred. At temperatures from 500–700°C, the decrease in after-exposure hardness of Condition A and H900 at longer exposure times was caused by a coarsening effect of copper-rich precipitates. A similar microstructural change was also responsible for the hardness of H1150 exposed at 700°C decreasing with increasing exposure time. Scanning electron microscopy (SEM) observations indicated that the matrix structures of Condition A and H900, when exposed at 600°C and above, exhibited lamellar recrystallized α -ferrite in the tempered martensite and the size and quantity of these lamellar ferrite phases increased with exposure time. X-ray diffraction (XRD) analyses showed that the reverted austenite phase in H1150 that formed during the over-aging treatment was stable and hardly affected by deformation at temperatures of 200–400°C. © 2003 Kluwer Academic Publishers

1. Introduction

Precipitation-hardening stainless steels have been widely used as structural components in various applications, such as nuclear, chemical, aircraft, and naval industries due to their excellent mechanical properties, good fabrication characteristics and excellent corrosion resistance. Of the former, 17-4 PH stainless steel is currently one of the most commonly used alloys [1]. Most of the previous investigations of 17-4 PH steels were focused on the effects of initial aging treatment on the microstructure and room-temperature mechanical properties [2–7]. Little work has been done on high-temperature mechanical properties of this alloy in various heat-treatment conditions. In general, the maximum strength and hardness values can be obtained after initially aging at 450–510°C, during which the precipitation of coherent copper-rich clusters occurs [1, 2]. Aging at a temperature above 540°C results in the precipitation of incoherent fcc copper-rich precipitates, lower strength and hardness, and enhanced toughness [1, 2]. At higher aging temperatures, around 580°C and above, a lamellar-like matrix structure and formation of reverted austenite phase are observed [3, 4, 7]. However, the lamellar-like matrix structure and the stability of reverted austenite under tensile loading at high temperatures have not been studied in detail. As some applications of 17-4 PH stainless steels involve

high-temperature exposure, it is thus important to characterize the high-temperature mechanical behavior and microstructural evolution of this alloy in various aged conditions. In particular, the influence of exposure at temperatures lower and higher than the initial aging temperature should be fully studied for various aged conditions so as to understand better the mechanical performance of this alloy in high-temperature environments.

The aim of this study is to characterize the effect of temperature on the tensile strength, hardness and microstructure of various heat-treated 17-4 PH stainless steels by systematic experiments at temperatures between 200 and 700°C.

2. Experimental procedures

The commercially available 17-4 PH stainless steel used in the current study was supplied by the vendor in the form of hot-rolled, solution-annealed bars. The chemical composition of this alloy (wt%) is 15.18 Cr, 4.47 Ni, 3.47 Cu, 0.65 Mn, 0.38 Si, 0.2 (Nb+Ti), 0.15 Mo, 0.03 S, 0.02 C, 0.016 P and Fe (balance). Three heat treatments were applied to the specimens, i.e. as-received unaged “Condition A,” peak-aged “Condition H900” and overaged “Condition H1150.” Details of the heat treatment procedures are given in Table I. The

* Author to whom all correspondence should be addressed.

TABLE I Heat treatment conditions of 17-4 PH stainless steels

| Condition | Treatment |
|-------------|------------------------------------------------|
| Condition A | 1,038°C (1,900°F) × 0.5 h → air cool |
| H900 | Condition A → 482°C (900°F) × 1 h → air cool |
| H1150 | Condition A → 621°C (1,150°F) × 4 h → air cool |

mechanical properties at room temperature for each aged condition are listed in Table II.

Tensile tests were conducted using a commercial closed-loop servo-hydraulic machine with an extension rate of 0.5 mm/min at room temperature, 200, 300 and 400°C in air. The tensile specimens have a cylindrical gage section of 6 mm in diameter and 18 mm in length. A commercial compact two-zone SiC element furnace was used to heat the specimens. Tensile strains were measured over a 12-mm gage length with a commercial direct-contact high-temperature extensometer. In high-temperature tensile tests, specimens from each condition were heated to the given temperature and held at temperature for different periods of time (0.25, 1, 4, 16 and 32 h) prior to testing. Hardness measurements were taken at room temperature on a Rockwell C scale tester for each material condition after exposure at 200, 300, 400, 500, 600 and 700°C for different periods of time. Hardness samples were circular disks of 12-mm diameter and 2-mm thickness and ten measurements were taken on each sample to obtain the average hardness value.

Microstructural analyses of the tensile specimens and hardness samples were conducted using scanning electron microscopy (SEM) and scanning transmission electron microscopy (STEM). Samples for SEM observation were prepared by etching with Fry’s reagent. Thin foils for TEM analysis were prepared by grinding 3-mm-diameter circular slices to a thickness of about 50 μm, then finally thinning by twin-jet electropolishing procedures. X-ray diffraction (XRD) was used for determination of the austenite phase.

3. Results and discussion

3.1. Effect of temperature and hold-time on tensile strength

Fig. 1 shows plots of high-temperature yield strength as a function of hold-time at three temperatures (200, 300 and 400°C) for each material condition. Fig. 1 indicates that the yield strength of each condition was reduced with increasing temperature except for Condition A at 400°C at times >16 for which strengths were greater than those at lower temperatures. The yield strength of Condition A tested at 400°C was increased to about

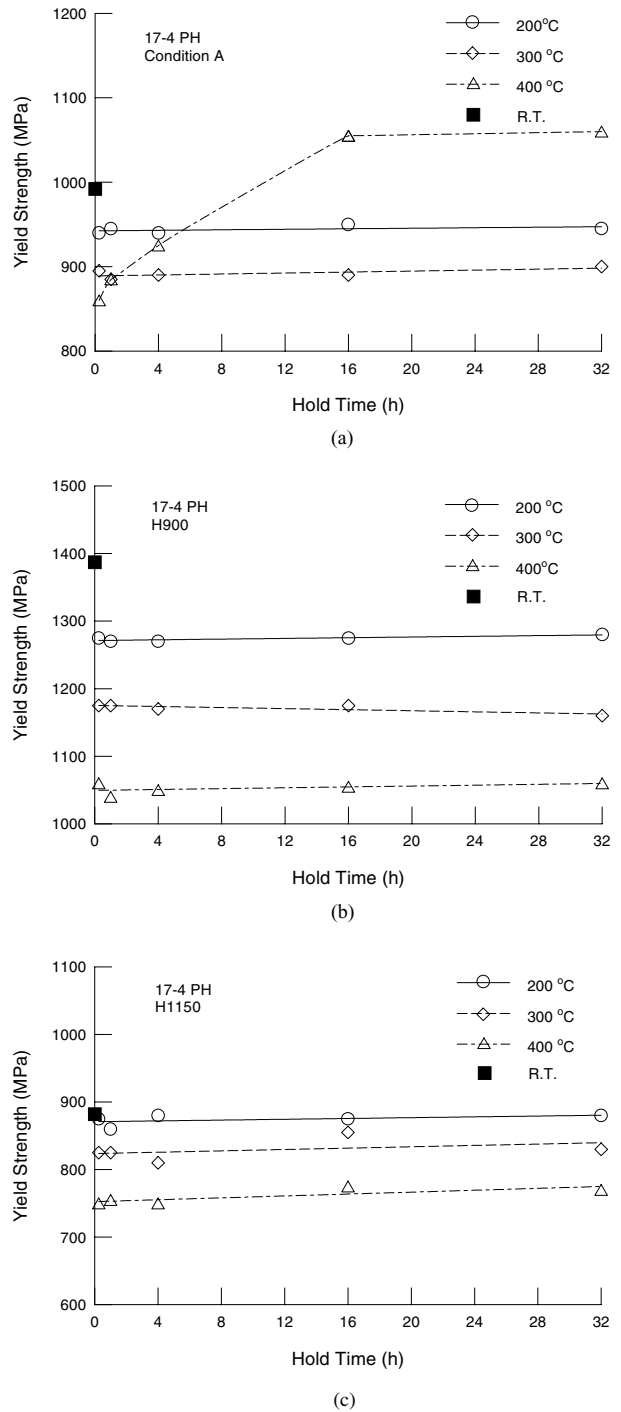


Figure 1 Variation of high-temperature yield strength with hold time for 17-4 PH in different conditions: (a) Condition A, (b) H900, and (c) H1150.

1050 MPa, which is equivalent to that of H900 condition at the same temperature. This resulted from a pronounced precipitation-hardening effect for Condition A tested at 400°C for longer hold-times. It can also be

TABLE II Room-temperature mechanical properties of 17-4 PH stainless steels in different aged conditions

| Condition | Ultimate tensile strength (MPa) | Yield strength (MPa) | Elastic modulus (GPa) | Elongation (in 25 mm) (%) | Hardness (HRc) | V-notch impact toughness (J) |
|-------------|---------------------------------|----------------------|-----------------------|---------------------------|----------------|------------------------------|
| Condition A | 1,018 | 992 | 199 | 13.4 | 32.0 | 67 |
| H900 | 1,414 | 1,387 | 223 | 12.5 | 44.5 | 21 |
| H1150 | 966 | 880 | 196 | 18.4 | 31.5 | 75 |

seen in Fig. 1 that the rank order of yield strength for the three conditions at a given temperature is generally: H900 > Condition A > H1150. Moreover, except for Condition A tested at 400°C, the yield strength of each condition at a given temperature was independent of the hold-time. This implies a lack of significant change in microstructure at a given high temperature with a hold-time ranging from 0.25 to 32 h. Previous investigations [4, 5] indicated that a certain long period of time was needed to complete the precipitation process for Condition A when age-treated at a temperature below 400°C. Therefore, it is suggested that the invariance of the yield strength with hold-time for Condition A tested at 200°C and 300°C could be attributed to the incompleteness of the precipitation process during the given hold-times. However, the microstructures of the two aged conditions, H900 and H1150, were unlikely to be affected by re-heating to a temperature below the original aging temperature such that the yield strengths of the two aged conditions at each given high temperature remained nearly unchanged with the hold-time. Microstructural analyses of the failed tensile specimens provided further support for the above arguments.

TEM analyses indicated that at a given high temperature between 200 and 400°C no visible change was found in the microstructures of H900 and H1150 conditions as the hold-time was increased from 0.25 to 32 h. For Condition A tested at 400°C with a 32 h hold-time, the microstructure (shown in Fig. 2) exhibited typical nearly-parallel martensite laths with a high density of dislocations. However, the fine, coherent copper-rich precipitates expected at this stage were not detected by TEM. This is due to the fact that the atomic scattering amplitude for electrons and atomic size are almost the same for Fe and Cu. At $\sin\theta/\lambda = 0$, the mean atomic scattering amplitudes for electrons in Fe and Cu are 6.4 and 6.8 Å, respectively [8], and the atomic radii of Fe and Cu are 1.24 and 1.28 Å, respectively [9]. Therefore, the bright-field images did not exhibit any obvious strain contrast around the precipitates and also

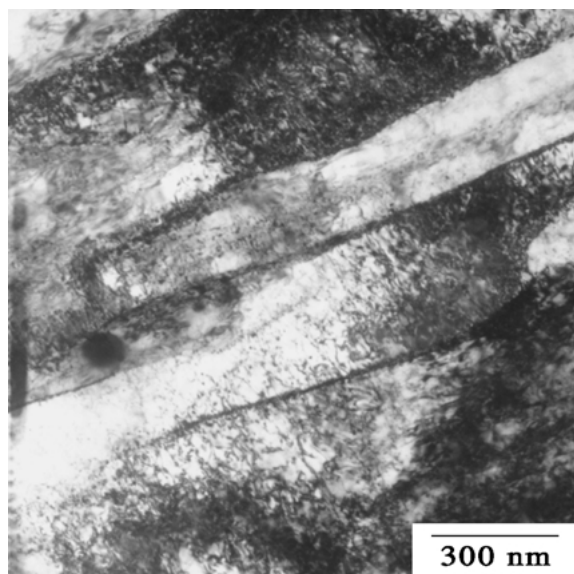


Figure 2 TEM micrograph of microstructure in Condition A of 17-4 PH stainless steel tested at 400°C with a 32 h hold-time.

no diffuse and distortion effects were observed in the diffraction patterns for the early stage of precipitation. Previous studies [3–5] have similarly shown that the copper-rich phase formed at the initial stage of precipitation process has a very fine and coherent structure and did not generate any obvious strain contrast around it such that it was difficult to detect by TEM. Nevertheless, it is assumed that the increase in yield strength for Condition A at 400°C to a value equivalent to that of the corresponding H900 condition was caused by the formation of fine, coherent copper-rich precipitates.

3.2. Effects of exposure temperature and time on hardness and microstructure

Fig. 3 shows plots of the after-exposure hardness for each condition with respect to the exposure time at various temperatures. It can be seen in Fig. 3 that the variation of the after-exposure hardness with the exposure time at 200 to 400°C for each condition generally exhibited a similar trend to that of the high-temperature yield strength. That is, the hardness was independent of the exposure time for a given material condition and exposure temperature, except for Condition A exposed at 400°C where the after-exposure hardness increased with exposure time as a result of a precipitation-hardening effect. Moreover, for a given material condition, the after-exposure hardness hardly varied with exposure temperature between 200–400°C except for Condition A at 400°C. TEM analyses indicated that no significant changes in precipitate size or dislocation density occurred for the three given materials after exposure at 200–400°C for 0.25 to 32 h except for Condition A at 400°C. Therefore, the reduction of the high-temperature yield strength with increasing temperature from 200 to 400°C for each condition might be attributed, mainly, to a decrease in atomic-bond strength due to the increasing atomic thermal vibration rather than microstructural change, except for Condition A at 400°C. The above results suggest that the trend of the variation of high-temperature tensile strength with the hold-time at a given temperature from 200 to 400°C for a 17-4 PH alloy could be obtained by simply measuring the after-exposure hardness.

In order to further understand the high-temperature properties of this alloy, the after-exposure hardness at higher exposure temperatures (500–700°C) was also measured in the present work. Fig. 3a indicates that, in comparison to the unexposed hardness value, the after-exposure hardness of Condition A at 500 and 600°C was increased at short exposure times and then gradually decreased with increasing exposure time, while at 700°C it generally decreased with an increase in exposure time. The increased hardness for Condition A heated at 500 and 600°C for less than 4 h could be attributed to the precipitation-hardening effect. The Cu-rich precipitates would become coarser, reducing the hardness at longer exposure times. At 700°C, the precipitates became so large that even at short exposure times the hardness value was consistently lower than the unexposed one. For unaged Condition A, the exposure process is similar to carrying out the aging treatment. Hence, it can be

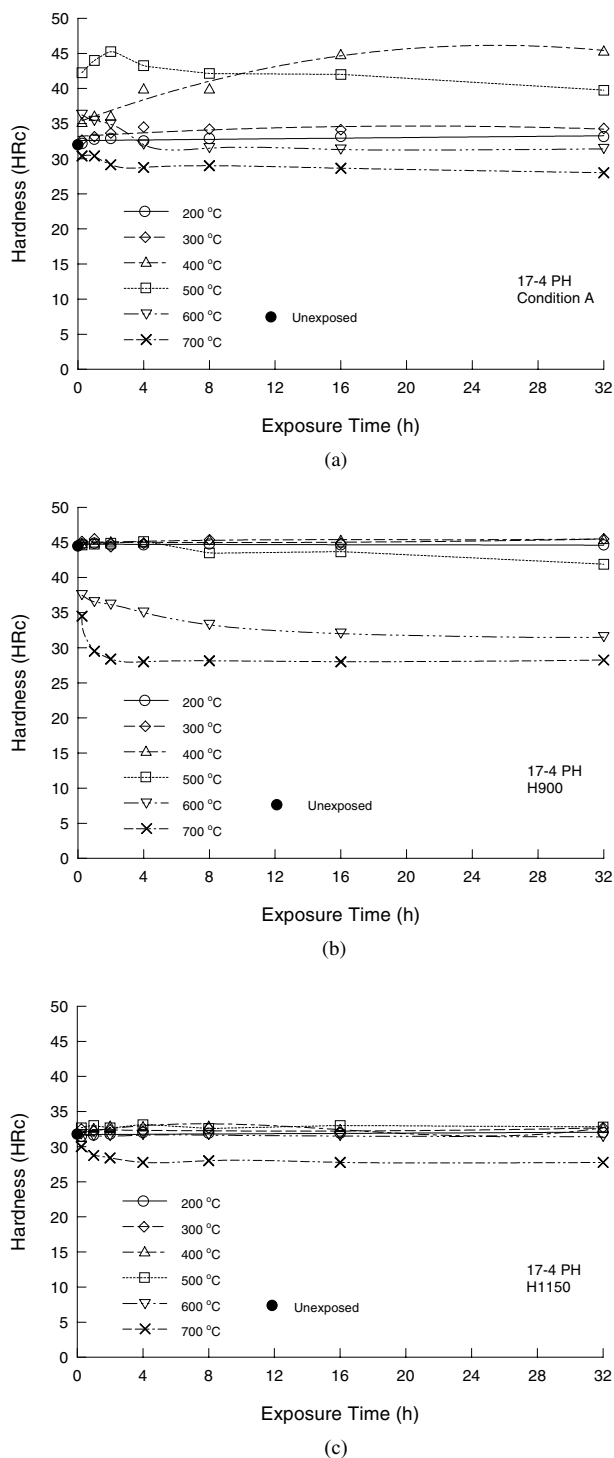


Figure 3 Variation of hardness with exposure temperature and time for 17-4 PH in different conditions: (a) Condition A, (b) H900, and (c) H1150.

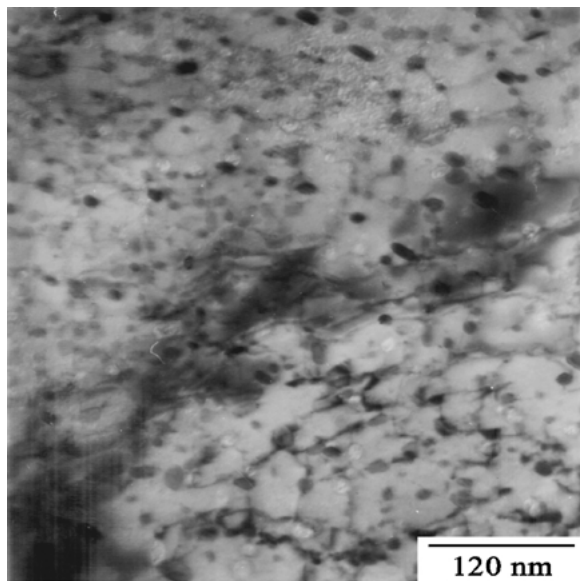
seen in Fig. 3a that the exposure time required to reach the maximum hardness decreased with increasing temperature, and in the temperature range of 400°C–600°C the peak value of the hardness also decreased with increasing temperature. These results are consistent with the typical age-hardening phenomena present in other alloys [10].

For the H900 condition, the after-exposure hardness at 500°C remained unchanged initially and decreased when the exposure time was longer than 4 h, as shown in Fig. 3b. The after-exposure hardness of H900 condi-

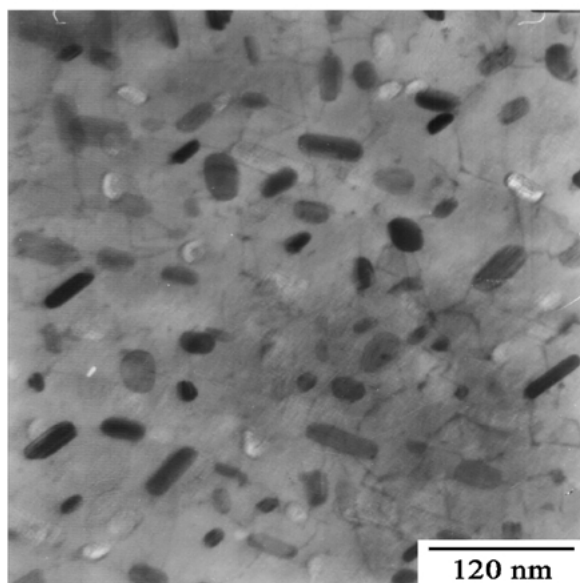
tion at 600 and 700°C, generally decreased to a steady value with increasing exposure time. The original H900 condition was generated by a peak-aging treatment at 482°C on specimens in Condition A, prior to any testing. Therefore, when exposed to a temperature above the original aging-treatment temperature, the precipitates in the H900 condition would gradually become coarser and cause the reduction in hardness at 500–700°C. As for Condition H1150, it can be seen in Fig. 3c that the after-exposure hardness was generally independent of the exposure time and stayed at a almost constant value at 500 and 600°C while at 700°C the hardness decreased to a steady value with an increase in exposure time. Apparently, exposure at 500 or 600°C, which are lower than the initial aging-treatment temperature, 621°C, does not cause the microstructure of H1150 condition to change such that the hardness remained constant regardless of the exposure time. At 700°C, the initial decrease in hardness was attributed to a coarsening of the precipitates.

TEM observations indicated that exposure at 500°C for 0.25 h does not significantly change the microstructure of Condition A except that a few precipitates in the visible size ranges were found at dislocation tangles. However, the major, fine, coherent and uniformly-distributed precipitates still could not be detected. Even so, the early increase in the hardness of Condition A when exposed at 500°C was believed to be caused by the formation of fine, coherent Cu-rich precipitates. Figs 4a and b show TEM micrographs of the microstructure of Condition A exposed at 600°C for 0.25 h and 32 h, respectively. Lots of homogenous Cu-rich precipitates can be seen in Fig 4a. These small precipitates strengthen the matrix to increase the hardness to a value superior to the unexposed (or unaged) one. With increasing exposure time, coarsening of the precipitates for Condition A at 500–700°C was observed and as shown in Fig. 4b, which should be compared with Fig. 4a. In addition, for a given exposure time, the precipitate size increased with temperature such that even with a short exposure time of 0.25 h at 700°C, the precipitates in Condition A had become rod shaped, like those in Condition A at 600°C with a 32 h exposure time (Fig. 4b). A similar variation in Cu-rich precipitate morphology was seen in H900 condition exposed at 500–700°C. Therefore, it was considered that the decrease in after-exposure hardness of H900 condition at 500–700°C with increasing exposure time could be also attribute to the coarsening of precipitates. For H1150 condition, TEM analyses indicated that the microstructure was barely changed at 200–600°C with exposure times ranging from 0.25 to 32 h. This explains why the after-exposed hardness in H1150 condition at 200–600°C was almost constant. For Condition H1150 exposed at 700°C, which is higher than the initial age-treatment temperature, 621°C, the precipitates became slightly larger and less dense leading to the reduction of hardness with increasing exposure time.

SEM micrographs of the original microstructures in Condition A and H1150 condition specimens are shown in Fig. 5. Fig. 5a shows that the matrix of Condition A consisted of equiaxial martensite laths within the prior



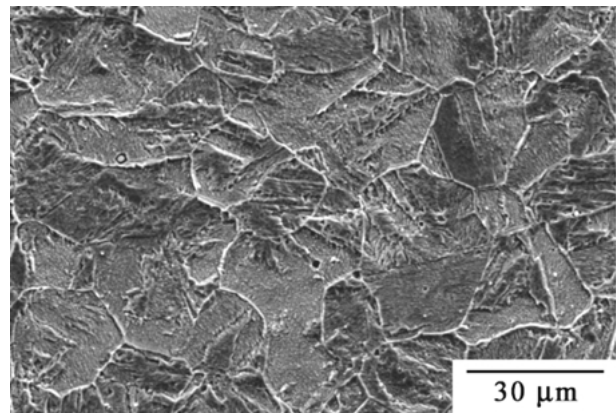
(a)



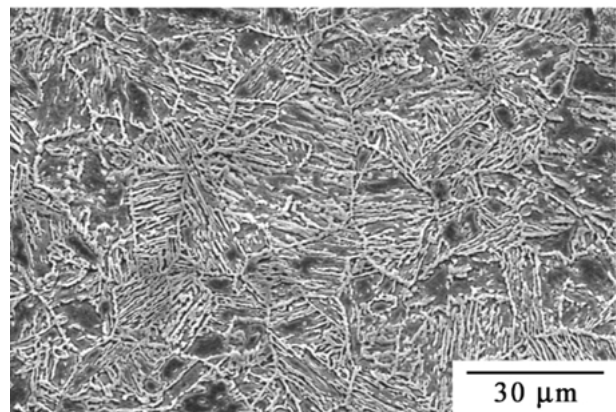
(b)

Figure 4 TEM micrographs of microstructure in Condition A of 17-4 PH stainless steel exposed at 600°C for (a) 0.25 h and (b) 32 h.

austenite grains and that the grain size was about 20–30 μm . For peak-aged H900 condition, the matrix structure was similar to that of the original Condition A, except that the profile of martensite laths within the prior austenite grains was clearer than that in Condition A. This is due to segregation or precipitation of the solute atoms at the lath and grain boundaries during the aging treatment such that these regions were easier to etch. However, the microstructural morphology of H1150 condition was apparently different from the other two conditions and possessed a lamellar-like structure (Fig. 5b) similar to the Windmännstätten structure [1], and unlike the typical tempered martensite structure. It can be seen in Fig. 5b that there is a large amount of a white lamellar phase, at least 40% in volume fraction, formed at martensite lath and grain boundaries. An earlier study by Antony [6] indicated that the microstructures of 17-4 PH, regardless of



(a)

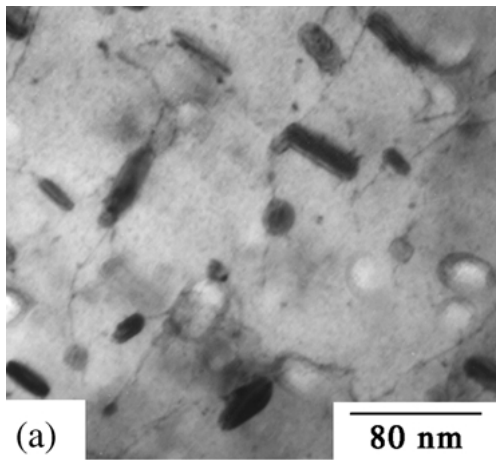


(b)

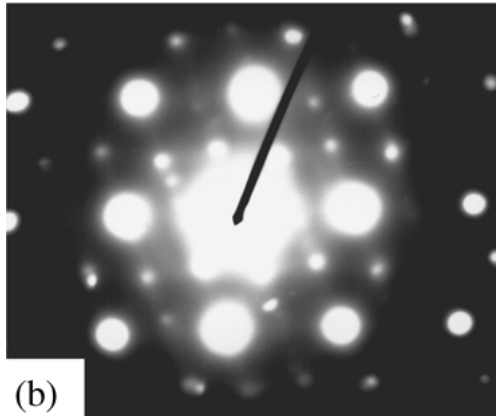
Figure 5 SEM micrographs of the original microstructure of 17-4 PH in (a) Condition A and (b) H1150.

aging conditions, were feathery transformation structures but not typical martensite or tempered martensite structures. Moreover, Xia *et al.* [7] indicated that a lamellar structure was present in a microstructure of 17-4 PH alloy aged at temperatures above 570°C and might be related to the formation of reverted austenite. However, in the present work, the amount of austenite in H1150 condition was about 6–9% by XRD analysis, far less than the 40% observed in Fig. 5b. As no data are available on the temperature of transformation of martensite to austenite, A_s , for 17-4 PH alloy, the A_s data in binary Fe-Ni alloys [11] were used as references in the current study. The plots of A_s for Fe-Ni alloys [11] indicated that the amount of austenite phase should be far less than that of ferrite phase at 621°C, even though the austenite phase may not exist at this temperature. Furthermore, TEM observations indicated that numerous ferrite laths in H1150 condition were recrystallized and large rod-like precipitates were also observed in these laths, as shown in Fig. 6. Fig. 6b showed the selected area diffraction (SAD) pattern taken from Fig. 6a. The pattern indicated that the recrystallized matrix was bcc α -ferrite and the precipitates were fcc Cu-rich phases. Consequently, it was considered that the white lamellar phase in H1150 condition was likely to be recrystallized α -ferrite phase formed in the tempered martensite during the aging treatment.

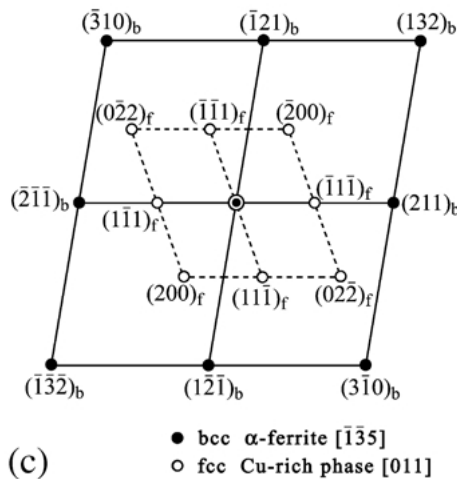
For each material condition exposed at 200–500°C for 0.25–32 h, no significant change in the



(a)



(b)



(c)

Figure 6 (a) TEM bright-field image of the recrystallized matrix in the original H1150 condition; (b) $[\bar{1}\bar{3}5]_{\alpha}$ and $[011]_{\text{Cu}}$ SAD pattern taken from (a); and (c) key to SAD pattern shown in (b).

microstructure was observed by SEM. However, at 600°C the matrix structures in Condition A and H900 exhibited the white lamellar phase for exposure times longer than about 2 h and the amount of white lamellar phase gradually increased with exposure time. The matrix structures in Condition A and H900 exposed at 600°C for 32 h were very similar to that in the original H1150 condition (Fig. 5b). The matrix structures of the three conditions exposed at 700°C are almost the same and a representative micrograph is given in Fig. 7. It can be seen in Fig. 7 that the size and quantity of the white lamellar phase increased significantly with exposure time to a plateau level beyond 4 h. Consequently, this

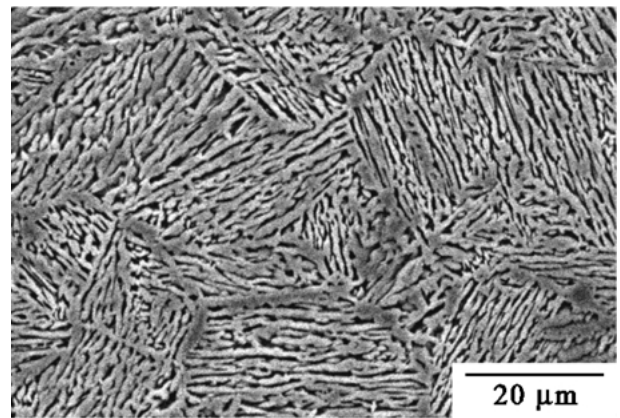


Figure 7 SEM micrograph of microstructure in H1150 condition of 17-4 PH stainless steel exposed at 700°C for 32 h.

variation of size and amount in lamellar ferrite phase was considered partially responsible for the decrease in the after-exposure hardness of Condition A and H900 exposed at 600 and 700°C as well as of H1150 exposed at 700°C .

3.3. Stability of reverted austenite

XRD analyses indicated that no austenite phase was present in solution-annealed Condition A and peak-aged H900 condition, but there was about 6–9% volume fraction of austenite in overaged H1150 condition. It was considered that this austenite phase was the reverted austenite formed during the over-aging treatment rather than retained austenite. Previous studies [3, 4] indicated that aging at a temperature above 600°C resulted in the segregation of an austenite stabilizer, copper, at lath boundaries such that the transformation temperature A_s in these regions would be lowered to facilitate the formation of austenite. This type of austenite could be retained on subsequent cooling to room temperature as the local M_s was reduced to be lower than room temperature by the segregation of copper atoms [3, 4]. After exposure at 200 – 400°C for 0.25–32 h, there was still no austenite phase detected in Condition A and H900. As for H1150 condition, the variation of reverted austenite content with exposure time in the temperature range 200 – 400°C is shown in Fig. 8. It

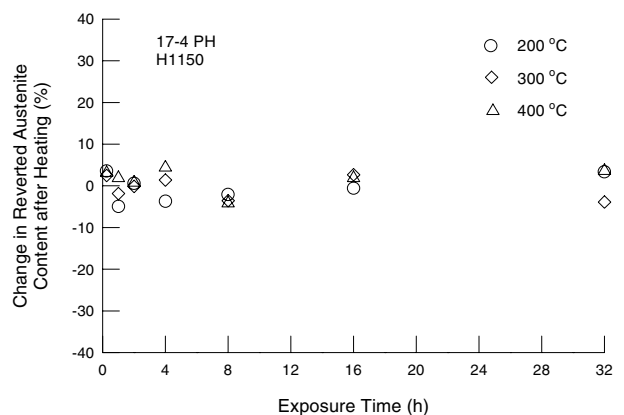


Figure 8 Change in reverted austenite content in H1150 condition of 17-4 PH stainless steel for various exposure temperatures and times.

TABLE III Difference in reverted austenite content of H1150 tensile specimens under various heating conditions

| Condition | Volume fraction of reverted austenite in grip section (%) (a) | Volume fraction of reverted austenite in gage section (%) (b) | Difference in reverted austenite content (%) [$=(b-a)/a \times 100\%$] |
|----------------|---------------------------------------------------------------|---------------------------------------------------------------|--------------------------------------------------------------------------|
| R.T. | 7.53 | 7.83 | 3.98 |
| 200°C × 0.25 h | 7.82 | 8.00 | 2.30 |
| 1 h | 7.39 | 7.70 | 4.19 |
| 4 h | 7.40 | 7.24 | -2.16 |
| 16 h | 7.25 | 7.31 | 0.83 |
| 32 h | 7.56 | 7.35 | -2.78 |
| 300°C × 0.25 h | 7.66 | 8.01 | 4.57 |
| 1 h | 7.78 | 7.90 | 1.54 |
| 4 h | 7.67 | 7.29 | -4.95 |
| 16 h | 5.87 | 6.10 | 3.92 |
| 32 h | 6.79 | 6.49 | -4.42 |
| 400°C × 0.25 h | 8.57 | 8.43 | -1.63 |
| 1 h | 8.78 | 9.10 | 3.64 |
| 4 h | 7.67 | 7.75 | 1.04 |
| 16 h | 7.78 | 7.72 | -0.77 |
| 32 h | 8.49 | 8.53 | 0.47 |

can be seen in Fig. 8 that the percentage change of the reverted austenite content between the after-exposure and original states varied in a relatively small range of -5-5% regardless of exposure temperature and time. In other words, the reverted austenite in the original H1150 condition was a stable phase and hardly affected by reheating at 200-400°C.

XRD analyses of the grip sections and areas in the gage sections near the fracture surfaces of the tensile specimens were also conducted to study the effect of deformation on variation in the austenite content. XRD results indicated that there was only small differences in the reverted austenite content between the grip and highly stressed gage sections for the H1150 specimens under various heating conditions, as listed in Table III. It can then be concluded that the reverted austenite phase in H1150 condition formed during the over-aging treatment was very stable and not significantly affected by the applied stresses at temperatures of 200-400°C.

4. Conclusions

1. For various heat-treated 17-4 PH stainless steels, the high-temperature yield strength of each condition was generally decreased with increasing temperature from room temperature to 400°C except for Condition A at 400°C at hold-times > 16 h.

2. At a given temperature between 200 and 400°C, the high-temperature yield strength of each condition was independent of the hold-time except for Condition A for which the yield strength at 400°C was increased with the hold-time, to a value equivalent to that of H900, due to a precipitation-hardening effect.

3. The variation of after-exposure hardness reflected the change of microstructure in various heat-treated 17-4 PH stainless steels after exposure at temperatures from 200-700°C for different periods of time.

4. For an aged 17-4 PH alloy, the hardness decreased with increasing exposure time at a temperature higher than the original age-treatment temperature due to a coarsening of Cu-rich precipitates.

5. In a 17-4 PH alloy, which was initially aged or reheated at a temperature above 600°C, the matrix exhibited a lamellar-like structure as a result of the formation of lamellar-type recrystallized ferrite in the tempered martensite. The size and amount of these lamellar ferrite phases increased with exposure time.

6. The reverted austenite in the original H1150 condition was a stable phase and hardly affected by the applied stresses at 200-400°C.

Acknowledgements

This work was funded by the National Science Council of the Republic of China (Taiwan) under Contract No. NSC-89-2216-E-008-018.

References

1. W. F. SMITH, "Structure and Properties of Engineering Alloys," 2nd ed. (McGraw-Hill, New York, USA, 1993).
2. H. J. RACK and D. KALISH, *Metall. Trans.* **5** (1974) 1595.
3. U. K. VISWANATHAN, S. BANERJEE and R. KRISHNAN, *Mater. Sci. Eng. A* **104** (1988) 181.
4. U. K. VISWANATHAN, P. K. K. NAYAR and R. KRISHNAN, *Mater. Sci. Tech.* **5** (1989) 346.
5. X.-S. ZANG, *Trans. Met. Heat Treat.* **12** (1991) 23 (in Chinese).
6. K. C. ANTONY, *J. Met.* **15** (1963) 922.
7. X.-L. XIA, Y.-Q. LI and D.-M. WU, *Material Science and Technology* **5** (1997) 106 (in Chinese).
8. J. W. EDINGTON, "Practical Electron Microscopy in Materials Science" (Van Nostrand Reinhold, New York, USA, 1976).
9. C. S. BARRETT and T. B. MASSALSKI, "Structure of Metals," 3rd ed. (McGraw-Hill, New York, USA, 1966).
10. R. E. REED-HILL and R. ABBASCHIAN, "Physical Metallurgy Principles," 3rd ed. (International Thomson Publishing, New York, USA, 1992).
11. F. W. JONES and W. I. PUMPHREY, *J. Iron Steel Inst.* **163** (1949) 121.

Received 21 March
and accepted 10 October 2002